

Table S1 PTRF siRNA sequences

PTRF siNC	5'-TGACCGGATTACCGTATCATGGCCT-3'
PTRF siRNA-1	5'-GCCGCAACTTTAAAGTCATGATCTA-3'
PTRF siRNA-2	5'-AGGAGTCCCGCGCAGAGCGTATCAA-3'

Table S2 primers for qPCR

PTRF-Forward	5'-GGCAGATCAAGAAGCTGGAGGT-3'
PTRF-Reverse	5'-CAGCGATTTGCTGATGCTCAGTT-3'
EGFRvIII-Forward	5'-GACAGCATAGACGACACCTTC-3'
EGFRvIII-Reverse	5'-CCTTATAGTCCTTATCATCGTC-3'
GAPDH-Forward	5'- GTTGCTGTAGCCAAATTCGTTGT-3'
GAPDH-Reverse	5'- GTTGCTGTAGCCAAATTCGTTGT-3'

Table S3 primers of PTRF promoter region for ChIP-PCR

1#Forward	5'-GAAGAGCTGATCAAGTCGGA-3'
1#Reverse	5'-TTGACCTCCAGCTTCTTGAT-3'
2# Forward	5'-AACTTGTAGCAGAACCGAAT-3'
2# Reverse	5'-CTGAATCACCCGCTATATCA-3'
3# Forward	5'-AAGTCATGATCTACCAGGTG-3'
3# Reverse	5'-ATTCGGTTCTGCTACAAGTT-3'
4# Forward	5'-TCCAAC TATTCCAACCATCC-3'
4# Reverse	5'-CTCGACAATATAGAGCGTGG-3'



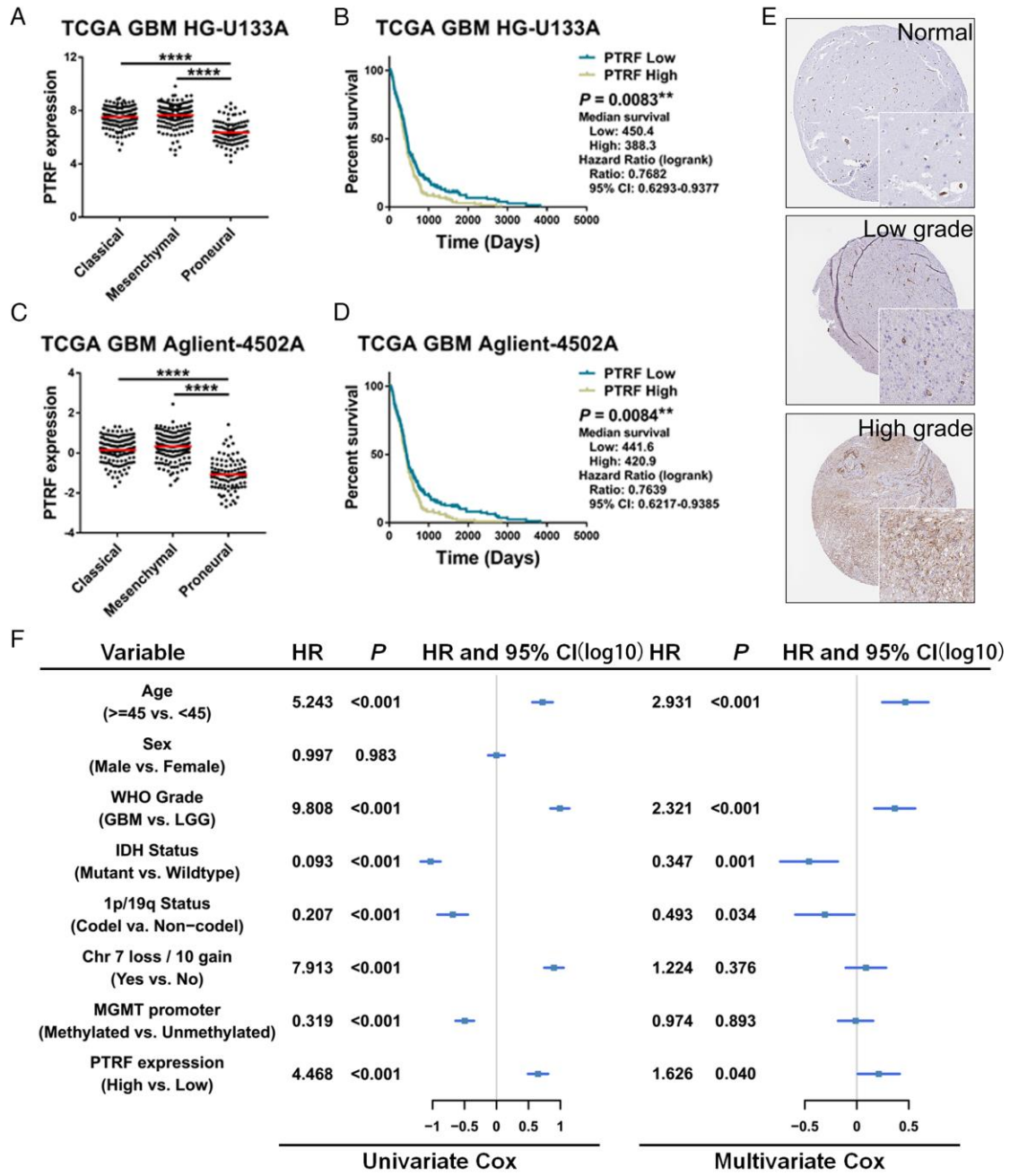


Fig S2

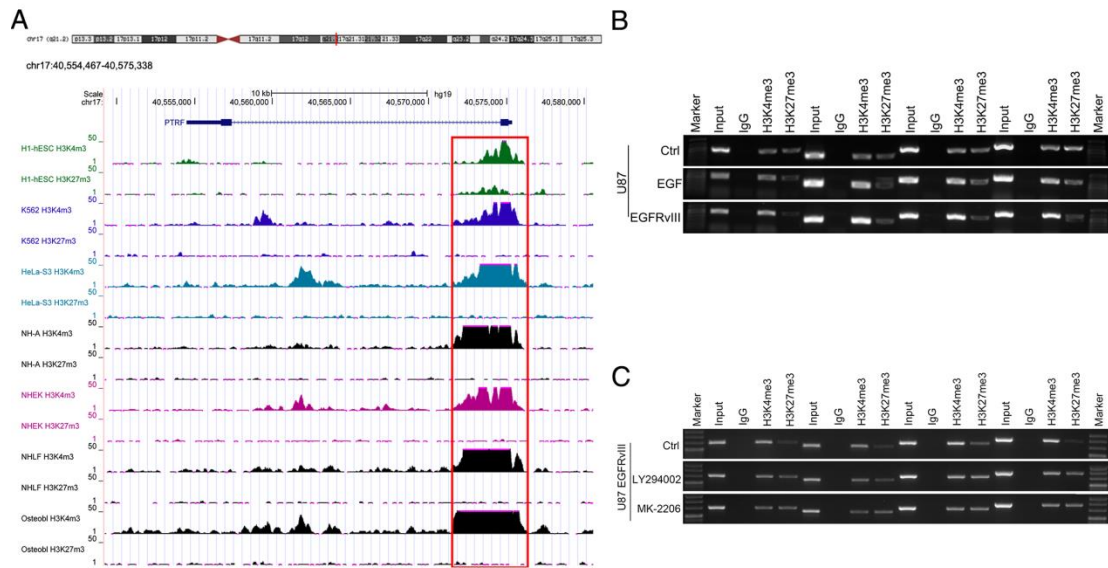


Fig S3

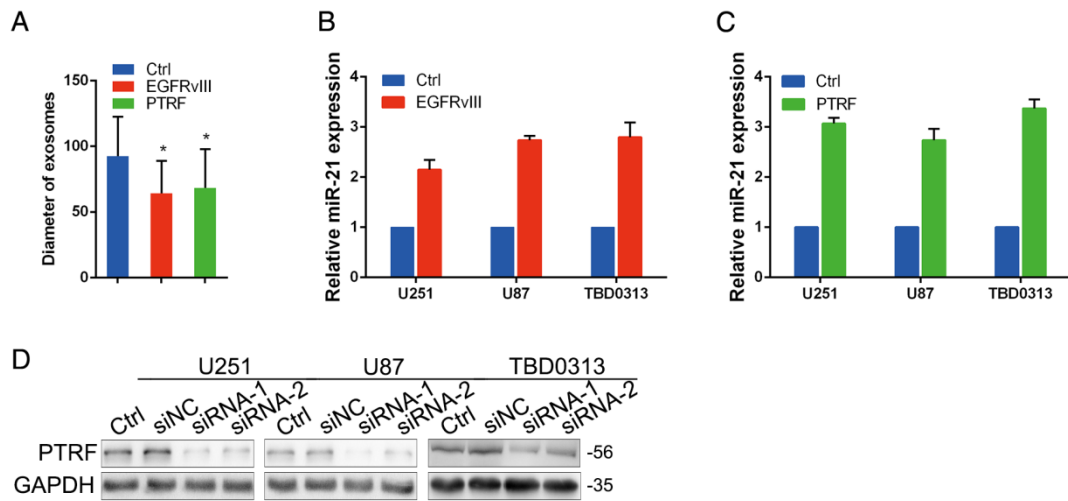


Fig S4

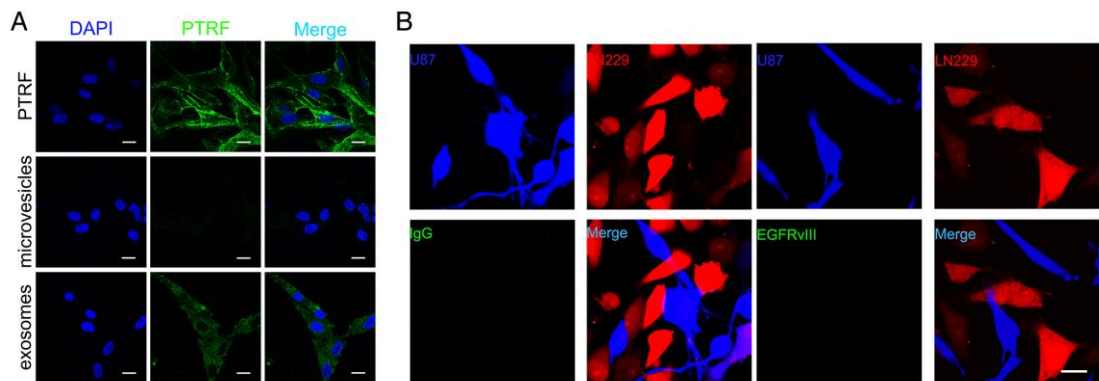


Fig S5

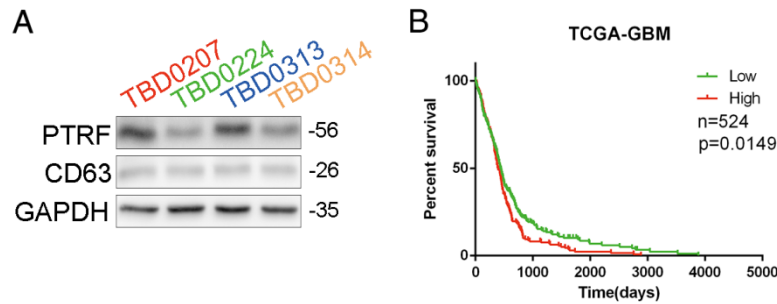


Fig S6

### legends

Fig S1. PTRF expression is positively associated with EGFR and EGFRvIII. (A) Similar to results of the DIA proteomic method (Fig. 1A), the TMT proteomic method was used to show that PTRF expression was increased by EGFRvIII overexpression. (B) Confocal microscopy showing that PTRF expression was increased in U87 cells stimulated with EGF or overexpressing EGFRvIII. Scale bar: 20  $\mu$ m. (C) Heatmap of CNV in 595 GBM samples from TCGA data showing that gene mutations in the PI3K/AKT pathway are not well correlated with EGFR amplification or mutations. (D) The CNVs of EGFR and PTRF in 595 GBM samples from TCGA data were not well correlated. Each point denotes a tumor sample ( $r=-0.035$ ,  $p=0.392$ ). (E) Heatmap of mRNA expression in 539 GBM samples from TCGA Affymetrix data showing that AKT1 and PTRF are positively associated with EGFR expression. (F) EGFR and PTRF expression patterns were positively correlated in 539 GBM samples. Each point denotes a tumor sample ( $r=0.304$ ,  $p<0.0001$ ).

Fig S2. PTRF is an independent biomarker in glioma diagnosis. (A and C) cDNA microarray analysis from the HG-U133A and Agilent-4502A were explored to show PTRF expression in GBMs. PTRF is enriched in patients with classical and mesenchymal GBM. (B and D) Kaplan-Meier curve showing that PTRF expression is associated with poor prognosis in glioma patients. (E) Immunohistochemistry of tissue microarray containing normal brain, low grade glioma and high grade glioma tissue sections. The representative PTRF stains are shown (<http://www.proteinatlas.org>). (F) Cox proportional hazards regression analyses of PTRF expression and other characteristics in relation to overall survival in GBM from TCGA cohort.

Fig S3. The PTRF promoter is enriched for H3K4me3 but not H3K27me3 in other cancer cells. (A) ChIP-seq data from UCSC Genome Browser tracks of the PTRF promoter region showing that the PTRF promoter is enriched with H3K4me3 but not H3K27me3 in various cancer cells. (B) Chip-PCR assays showing that H3K4me3 exhibited increased binding and H3K27me3 exhibited decreased binding to the PTRF promoter after EGFRvIII treatment. (C) Chip-PCR assays showing that H3K4me3 exhibited decreased binding and H3K27me3 exhibited increased binding to the PTRF promoter after LY294002 and MK-2206 treatment.

Fig S4. PTRF promotes exosome formation. (A) Exosomes isolated from GBM cells transduced with EGFRvIII or PTRF were smaller than those isolated from the control group, as measured by dynamic light scattering. (B) Exosomes were isolated from the supernatants of U87, U251 and TBD0313 cells transduced with vector or EGFRvIII. mRNA was then extracted, and the qRT-PCR assay was performed, showing that miR-21 expression was increased. (C) qRT-PCR showing that miR-21 expression was

increased after PTRF overexpression. For (B) and (C), U6 was used as the negative control. (D) After silencing PTRF by PTRF siRNA-1 and PTRF siRNA-2, the inhibitory efficiency of each siRNA was determined by western blot. Among these sequences, PTRF siRNA-1 showed the best efficiency to knock down PTRF. GAPDH served as the negative control.

Fig S5. PTRF induces intercellular communication via exosomes. (A) Microvesicles and exosomes isolated from the supernatant of U251 cells transduced with PTRF-EGFP were added to U87 cells for 24 hours, and confocal microscopy showed that exosomes, but not microvesicles, carried PTRF-EGFP. The scale bar corresponds to 20  $\mu$ m. (B) LN229 cells expressing RFP and U87 cells expressing EGFP were mixed together for 96 hours. Confocal microscopy was used to detect EGFRvIII staining as the negative control. Blue represents U87 cells, red represents LN229 cells and green represents stained IgG or EGFRvIII. The scale bar corresponds to 20  $\mu$ m.

Fig. S6. PTRF down-regulation is detectable after surgery. (A) PTRF and CD63 expression was detected in four primary cell lines by western blot (TBD0207, TBD0224, TBD0313, TBD0224 and TBD0314). Among these cell lines, TBD0207 and TBD0313 showed higher PTRF expression, while TBD0224 and TBD0314 showed lower PTRF expression. CD63 expression was not significantly different among the four cell lines. (B) The PTRF/CD63 ratio in TCGA microarray data was used to evaluate the overall survival of GBM patients. Kaplan-Meier survival curve analysis showed that the PTRF/CD63 ratio was positively related to the poor prognosis of GBM patients ( $p=0.0149$ ).